

## Electronic Supplementary Information

### **Table of Content:**

*1. General Methods*

*2. Characterization of the electrode materials*

*3. Electrochemical characterization of the electrodes*

*4. Electrochemical characterization of the SSCs*

## 1. General Methods

**Table S1** The production yield of carbon materials.

	raw mass (mg)	mass after carbonization (mg)	mass after activation (mg)	production yield (%)
LPC-600	1446	514	203	14
CPC-600	1576	614	205	13

**Materials Characterization:** All reagents are commercial and were used as received. The morphology of the samples was analyzed by scanning electron microscopy (SEM; SU-70, Hitachi) equipped with an energy-dispersive X-ray (EDX) spectrometer. The X-ray powder diffraction (XRD) spectra were collected on a Rigaku D/max2600 X-ray diffractometer. X-ray photoelectron spectroscopy (XPS) tests were performed on a Thermo ESCALAB 250XI instrument using monochromatic AlK $\alpha$ -ADES (ht=1486.6 eV) as the source. The Brunauer-Emmett-Teller (BET) surface area were performed by N<sub>2</sub> adsorption measurements at 77.3 K using a Nova 2000E.

## 2. Characterization of the electrode materials

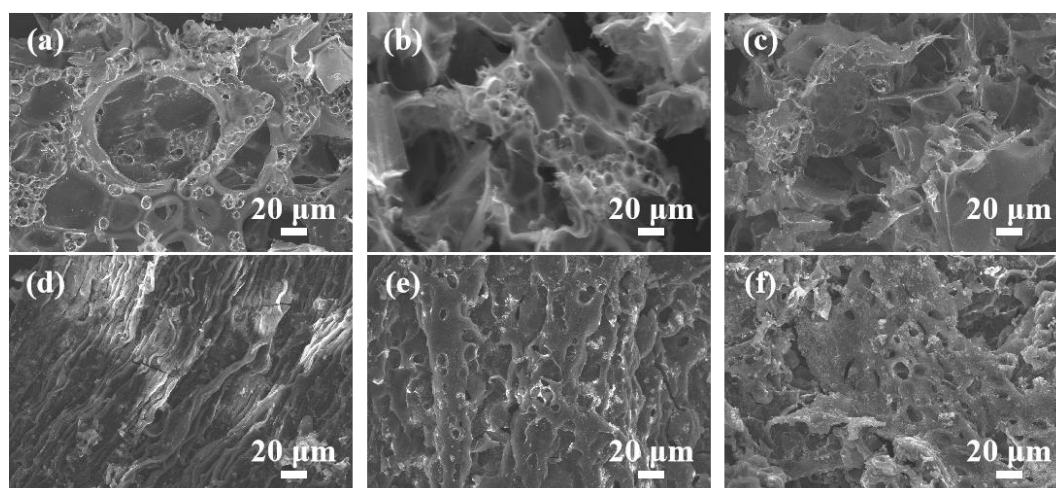


**Fig. S1** The SEM images of (a) CPC-500, (b) CPC-600, (c) CPC-700 and (d) LPC-500, (e) LPC-600, (f) LPC-700.

**Table S2** Element contents of the samples.

Elemental analysis			
Samples	C (wt%)	N (wt%)	O (wt%)
CPC-500	73.7	6.1	20.2
CPC-600	74.9	7.0	18.1
CPC-700	79.7	7.5	12.8
LPC-500	72.5	6.3	21.2
LPC-600	80.7	7.9	11.4
LPC-700	80.0	9.7	10.3

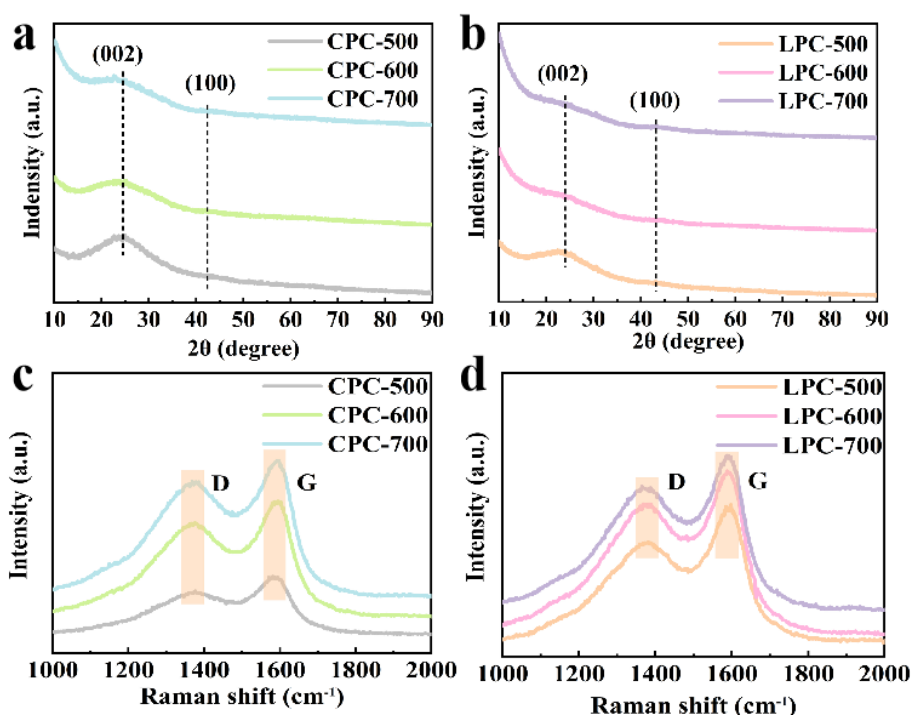


**Fig. S2** (a, b) The XRD patterns of CPC-x and LPC-x samples. (c, d) The Raman spectrum of CPC-x and LPC-x samples.

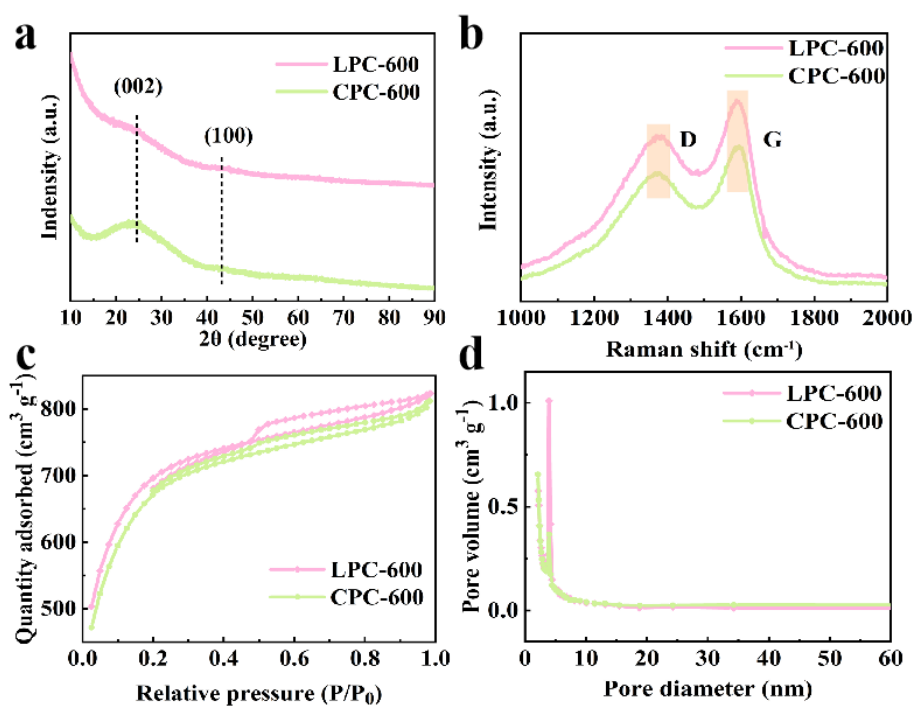


**Fig. S3** (a) The XRD patterns, (b) Raman spectrum, (c) N<sub>2</sub> adsorption-desorption isotherms and (d) pore size distributions of CPC-600 and LPC-600 samples.

**Table S3** The XPS test data of CPC-600.

Chemical element	Name	Peak BE	Area(P)CPS.ev	Atommic%
C	C=C	284.00	21304.77	57.61
	C-N	285.20	4363.91	11.80
	C-OH	285.97	4710.15	12.74
	C=O	288.10	6603.80	17.86
N	N-6	398.60	519.42	44.09
	N-5	399.80	328.83	27.91
	N-X	402.60	329.80	28.00
O	C=O	531.27	4389.67	29.40
	C-OH	532.20	4524.19	30.31
	C-O-C	532.90	6014.50	40.29

**Table S4** The XPS test data of LPC-600.

Chemical element	Name	Peak BE	Area(P)CPS.ev	Atomic%
C	C=C	284.10	21983.40	71.85
	C-N	285.70	2914.74	9.53
	C-O	286.50	2925.88	9.56
	C=O	288.10	2771.04	9.06
N	N-6	398.10	438.00	39.36
	N-5	399.20	328.93	29.56
	N-X	402.20	346.01	31.09
O	C=O	531.50	5155.95	32.10
	C-OH	532.20	10907.98	67.90

### 3. Electrochemical characterization of the electrodes

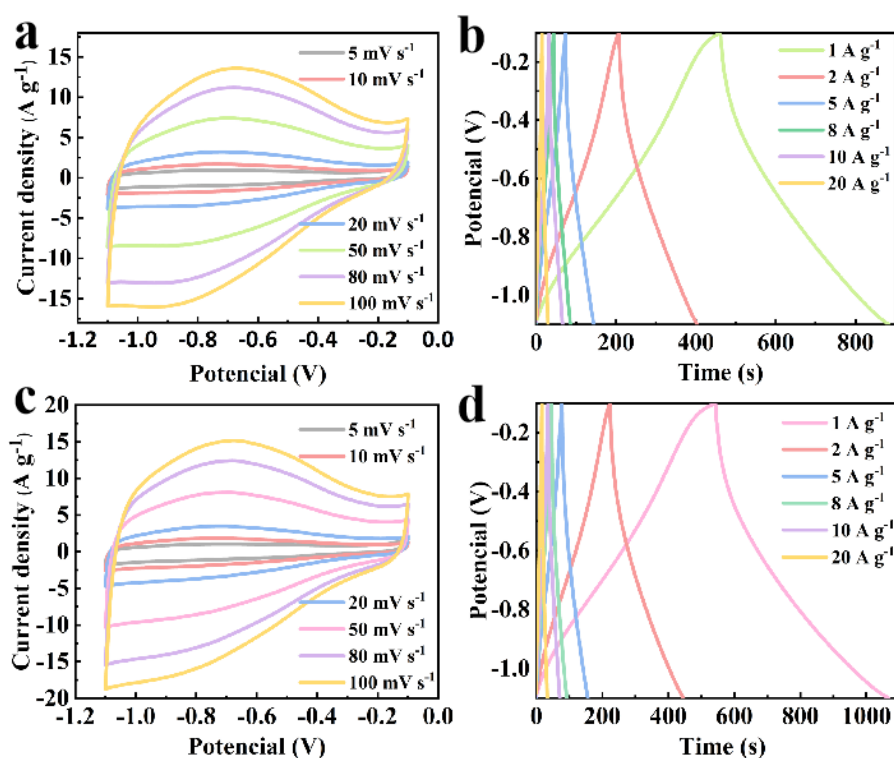


**Fig. S4** (a, c) The CV curves of CPC-600 and LPC-600. (b, d) The GCD curves of CPC-600 and LPC-600.

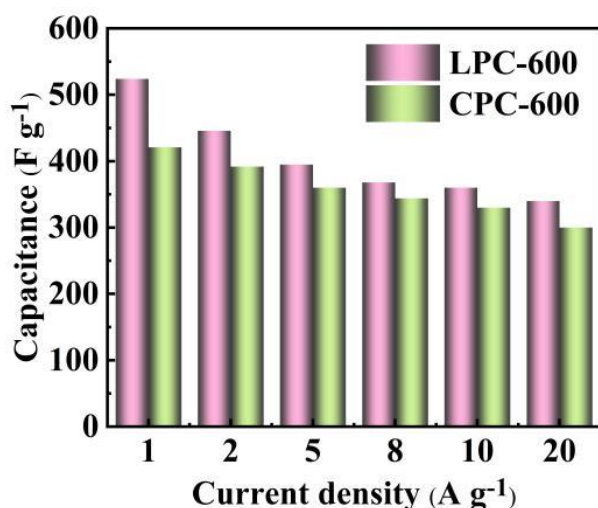


Fig. S5 The Cs at different current densities of LPC-600 and CPC-600.

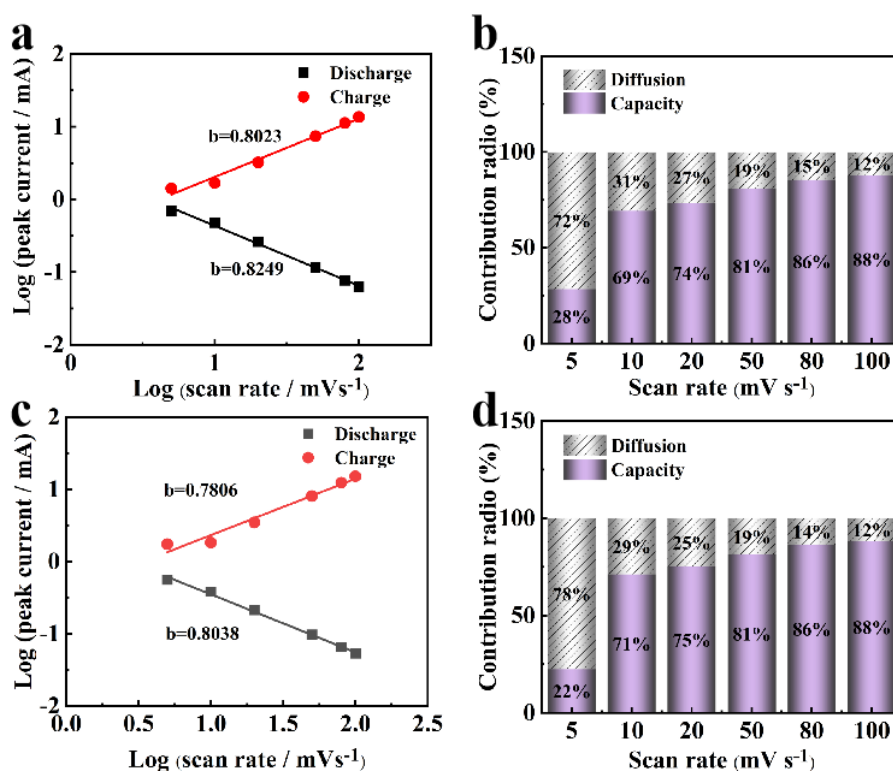


Fig. S6 (a, c) Power law dependence of positive and negative peak currents at different scan rates from 5 to 100 mV s<sup>-1</sup> for CPC-600 and LPC-600. (b, d) Contribution of CPC-600 and LPC-600 capacitance control capacity at different scan rates.

From Fig. S6a, it can be calculated that the  $b$  value of CPC-600 is between 0.5 ~ 1, which indicates that the two mechanisms coexist. Similarly, from Fig. S6c, it can be calculated that the  $b$  value of LPC-600 is less than CPC-600 and is also between 0.5 ~

1. This shows that the LPC-600 electrode has a larger proportion of pseudocapacitance, but the surface control dynamics still dominate. As shown in Fig. S6b and d, as the sweep speed increases, so does the contribution of the surface-controlled electrical double-layer capacitors. The maximum surface control ratio of CPC-600 and LPC-600 reached 88%, which indicates that they have good cycle stability and rate performance.

The volumetric capacitive performance of CPC-500, CPC-600, CPC-700, LPC-500, LPC-600 and LPC-700 is  $142.5 \text{ F cm}^{-3}$ ,  $210.5 \text{ F cm}^{-3}$ ,  $177.5 \text{ F cm}^{-3}$ ,  $196.0 \text{ F cm}^{-3}$ ,  $262.0 \text{ F cm}^{-3}$  and  $222.5 \text{ F cm}^{-3}$ .

#### 4. Electrochemical characterization of the SSCs

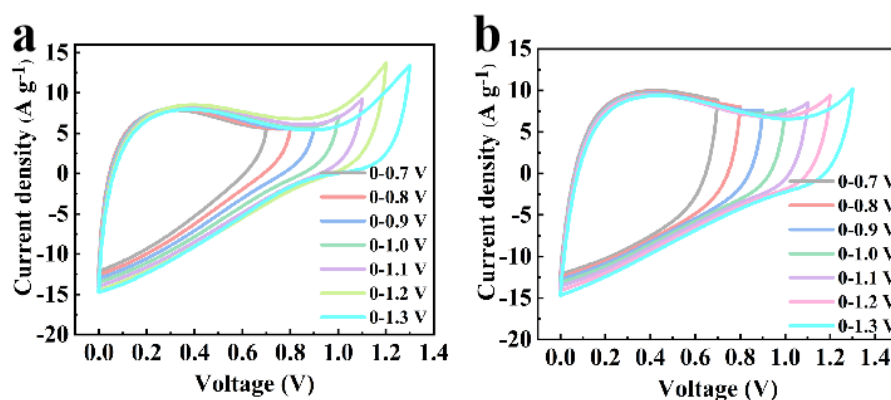


**Fig. S7** Electrochemical performance of supercapacitors in a 6 M KOH electrolyte. (a, b) The CV curves of CPC-600 SSC and LPC-600 SSC at  $50 \text{ mV s}^{-1}$  at various voltage regions (0.7 to 1.3 V).

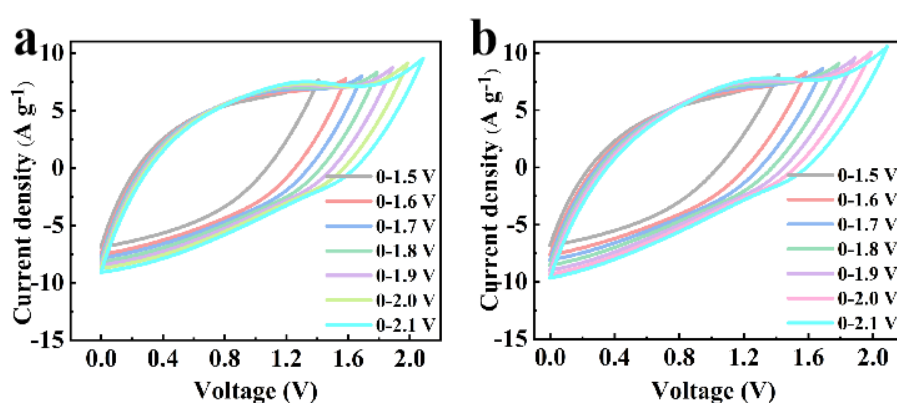


**Fig. S8** Electrochemical performance of supercapacitors in a 1 M  $\text{Na}_2\text{SO}_4$  electrolyte. (a, b) The CV curves of CPC-600 SSC and LPC-600 SSC at  $50 \text{ mV s}^{-1}$  at various voltage regions (1.5 to 2.1 V).

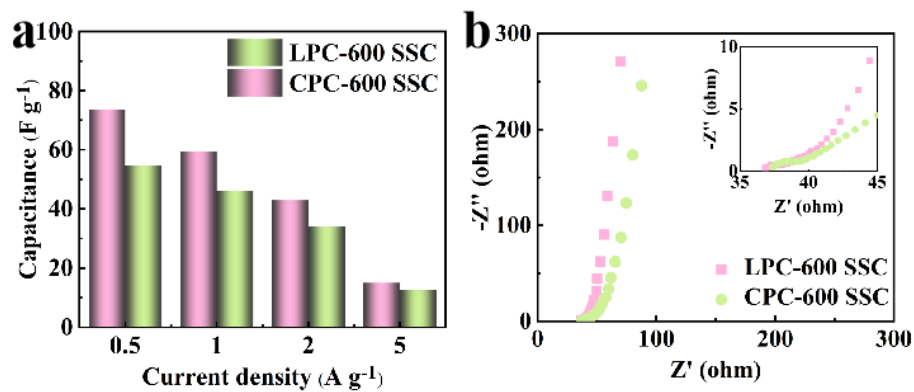


**Fig. S9** (a) The  $C_s$  at different current densities of CPC-600 SSC and LPC-600 SSC. (b) Nyquist diagram of the CPC-600 SSC and the LPC-600 SSC in 1 M Na<sub>2</sub>SO<sub>4</sub>.

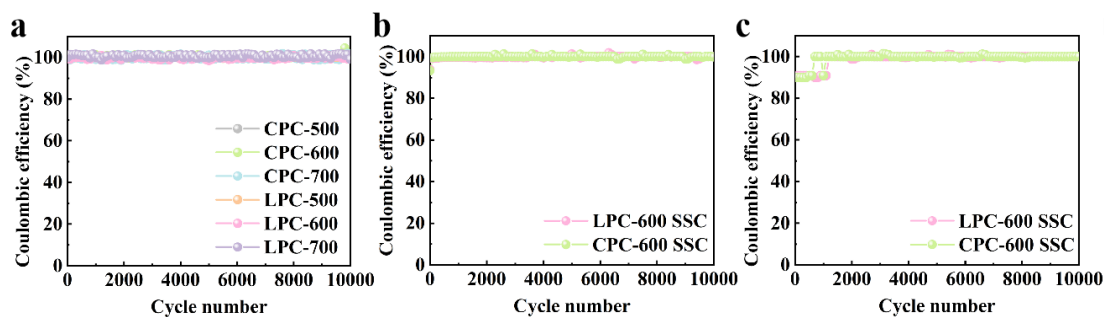


**Fig. S10** The Coulomb efficiency of (a) all samples in 6 M KOH in a three-electrode system, (b) two SSCs in 6 M KOH and (c) two SSCs in 1 M Na<sub>2</sub>SO<sub>4</sub>.